BBAA VI International Colloquium on:
Bluff Bodies Aerodynamics & Applications
Milano, Italy, July, 20–24 2008

AN ANALYTICAL MODEL FOR THE LIFT ON A ROTATIONALLY OSCILLATING CYLINDER

Isam Janajreh[⋆] and Muhammad Hajj[†]

[⋆]Department of Mechanical Engineering
Masdar Institute of Science and Technology, MASDAR, Abu Dhabi, UAE
e-mail: janajreh@mit.edu

[†]Department of Engineering Science and Mechanics
Virginia Polytechnic Institute and State University, Blacksburg, VA 24061, USA
e-mail: mhajj@vt.edu

Keywords: Circular Cylinder, Rotational Oscillations, Lift, Nonlinear Coupling, Higher-Order Spectra, Bispectrum, Trispectrum

An analytical model to predict the lift on a circular cylinder undergoing forced rotational oscillations in the lock-on regime is developed. Lift coefficient data are obtained from numerical simulations of the flow field over a rotationally oscillating circular cylinder. Higher-order spectral analysis, namely, the trispectrum, is applied to the data to characterize the nonlinear coupling between the vortex shedding frequency and its third harmonic. Based on this analysis, it is determined that the forced van der Pol equation should be used to model the lift coefficient on the rotationally oscillating cylinder in the lock-on regime. The developed analytical model for the lift is validated by comparing its time and frequency domain characteristics with those of the numerically simulated data.

1 Introduction

Oscillating drag and lift forces on circular cylinders are directly related to the vortex shedding pattern in their wakes. In various applications, the interest would be in reducing these forces, reducing vortex induced-vibrations, or augmenting the lift component. Different forcing conditions have been shown to significantly affect the wake pattern and associated forces on the cylinders. One such condition is the rotational oscillation forcing which has been shown to effectively modify the wake characteristics. Studies by Tokumaru and Dimotakis[1], Lu and Sato[2] and Chou[3] on rotationally oscillating cylinders revealed a significant drag reduction under specific forcing conditions. Choi et al.[4] showed that the maximum amplitude of the lift coefficient is increased in the lock-on region.

The optimal approach to assess effects of cylinder forcing on the wake structure and lift and drag forces would be a time-domain numerical simulation of the fluid flow and the structure's motions. On the other hand, and for different purposes such as optimization of the forcing parameters, analytical models have been proposed as a more efficient alternative for determining

fluctuating forces on oscillating circular cylinders. One of the first models proposed for vortex-induced vibrations of circular cylinders is the one by Hartlen and Currie[5]. In that model, the lift, represented by a Rayleigh equation, is linearly coupled to the cylinder's motion. Using a combination of approximate solutions of the Rayleigh and van der Pol equations and amplitude and phase measurements of higher-order spectral moments, Nayfeh, Owis and Hajj [6] showed that the lift coefficient, l, on stationary circular cylinders should be modeled by the self-excited van der Pol equation. The extension of such models to develop analytical models for forces on oscillating cylinders would be very beneficial for modeling vortex-induced vibrations, drag reduction or lift augmentation.

In this work, we develop an analytical model for the prediction of the lift on a rotationally oscillating cylinder. Numerical simulations are performed to generate a database from which parameters for the developed models are determined. Amplitude and phase measurements from higher-order spectral parameters are matched with approximate solutions of the models to characterize the nonlinearities in the model and determine these parameters.

2 Numerical Simulation

Direct Numerical Simulations of the unsteady incompressible Navier-Stokes equations for different cases of the flow over a rotationally oscillating circular cylinder were performed. All simulations were performed at $Re = U_\infty D/\nu$ = 100. The computational domain extended 5 cylinder diameters upstream, 10 diameters cross-stream on each side and 20 diameters downstream. The domain was staggered by multiple blocks with a quadratic cell type mesh, in order to provide more faces and to enhance the cell communication and computational accuracy. The cylinder wall was padded with a boundary layer mesh to accurately capture the viscous layer. The first cell thickness is 0.0002D and with a linear growth rate of 1.05. Imposed cylinder rotations were determined by two parameters, namely, the nondimensional amplitude, $\dot{\theta}_{max}D/2U_\infty$ = 0.5 where $\dot{\theta}_{max}$ is the maximum forcing angular velocity, and the forcing frequency $f_f U_\infty/D = 0.1643$, where f_f is the dimensional forcing frequency.

3 Higher-Order Spectral Moments

Traditional signal processing techniques used in data analysis are based on second-order statistics, such as the power spectra which are the Fourier transforms of the second-order correlation functions. These quantities yield an estimate of energy content of the different frequency components in a signal or the coherence between equal frequency components in two signals. In many cases, higher-order spectral moments can be used to obtain more information from signals or time series. In nonlinear systems, frequency components interact to pass energy to other components at their sum and/or difference frequency. Because of this interaction, the phases of the interacting components are coupled. This phase coupling can be used for the detection of nonlinear interactions between frequency components in one or more time series. Faced with an unknown system in terms of its nonlinear characteristics, these moments can be applied to identify quadratic and cubic nonlinearities. The bispectrum [7, 8, 9], which is the next higher-order moment to power spectrum, has been established as a tool to quantify the level of phase coupling among three frequency components and thus identify quadratic nonlinearities. Of particular interest to this work is the trispectrum [10], which is the next higher-order moment to the bispectrum, and which is used to detect and characterize cubic nonlinearities expected to be a part of the lift coefficient.

The higher-order spectral moments, introduced above, are multi-dimensional Fourier trans-

forms of higher-order statistical moments. If $x(t)$ is a real random process and its moments up to order n are stationary, one could define the n^{th}-order moment function

$$m_n(\tau_1, ..., \tau_{n-1}) = E\{x(t)x(t+\tau_1)...x(t+\tau_{n-1})\} \tag{1}$$

where $E\{\}$ represents ensemble averaging and $\tau_1, ..., \tau_{n-1}$ represent time differences. By Fourier transforming the second, third and fourth-order moment functions, one obtains, respectively, the auto-power spectrum, auto-bispectrum and auto-trispectrum [10]. The hierarchy of higher-order moment spectra is then expressed as

$$S_{xx}(f) = \lim_{T\to\infty} \frac{1}{T} E[X_T^*(f)X_T(f)] \tag{2}$$

$$S_{xxx}(f_1, f_2) = \lim_{T\to\infty} \frac{1}{T} E[X_T^*(f_1)X_T^*(f_2)X_T(f_1+f_2)] \tag{3}$$

and

$$S_{xxxx}(f_1, f_2, f_3) = \lim_{T\to\infty} \tfrac{1}{T} E[X_T^*(f_1)X_T^*(f_2)X_T^*(f_3)X_T(f_1+f_2+f_3)] \tag{4}$$

where $X_T(f)$ is the Fourier transform of $x(t)$ defined over a time duration T, and the superscript * is used to denote complex conjugate. The higher-order spectral moments and their normalized counterparts are capable of identifying nonlinear coupling among frequency components and quantifying their phase relations[7, 8, 9]. In this work, we will stress the use of the auto-trispectrum to determine the phase relation between the vortex shedding component and its third harmonic. This relation will be used in determining the parameters of the proposed analytical model.

4 Lift Modeling

The lift coefficient on a circular cylinder undergoing forced rotational oscillations in the lock-on regime is modeled by the van der Pol oscillator that is externally excited by a harmonic function and represented by

$$\ddot{l} + \omega_s^2 l^2 - \epsilon\mu_v \dot{l} + \epsilon\alpha_v l^2 \dot{l} = \epsilon F cos(\Omega t + \tau_e) \tag{5}$$

where ω_s is the shedding frequency, μ_v and α_v represent the linear and nonlinear damping coefficients, and F and τ_e are respectively the amplitude and phase of the external harmonic force. The forcing F, μ_v and α_v are scaled to the same orderϵ.

Using the method of multiple scales [11, 12], an analytical approximate solution is derived for Eq. 5 under the primary resonance condition

$$\Omega = \omega_s + \epsilon\sigma \tag{6}$$

where σ is the external detuning parameter. The approximate solution is written as

$$l(t) \approx \quad acos(\Omega t + \tau_e - \gamma) + \tfrac{a^3\alpha_v}{32\omega_s} cos(3(\Omega + \tau_e - \gamma) + \tfrac{\pi}{2}) \tag{7}$$

where γ is given by

$$\gamma = \epsilon\sigma t + \tau_e - \beta \tag{8}$$

In Eq. 7, the amplitude a and phase γ are governed by

$$\begin{aligned} \dot{a} &= \tfrac{\mu_v}{2} a - \tfrac{\alpha_v}{8} a^3 + \tfrac{F}{2\omega_s} sin\gamma \\ a\dot{\gamma} &= a\sigma - \tfrac{F}{2\omega_s} cos\gamma \end{aligned} \tag{9}$$

An examination of the expression for γ reveals its dependency on the phase of excitation, τ_e, and the phase of the response, β. When a and γ are constants in Eq. 9, i.e., for steady-state oscillations, the solution given in Eq. 7 represents a periodic motion which can be written in complex form as

$$l(t) \approx \frac{a}{2}\{e^{i(\Omega t+\tau_e-\gamma)} + e^{-i(\Omega t+\tau_e-\gamma)}\} + \frac{a^3\alpha_v}{64\omega_s}\{e^{3i(\Omega t+\tau_e-\gamma)+i\frac{\pi}{2}} + e^{-3i(\Omega t+\tau_e-\gamma)-i\frac{\pi}{2}}\} \tag{10}$$

The Fourier transform of $l(t)$ represented by $L(\omega)$ is then given by

$$\begin{aligned} L(\omega) \approx \; & \frac{a}{2}\{e^{i(\tau_e-\gamma)}\delta(\omega-\Omega) + e^{-i(\tau_e-\gamma)}\delta(\omega+\Omega)\} \\ & + \frac{a^3\alpha_v}{64\omega_s}\{e^{3i(\tau_e-\gamma)+i\frac{\pi}{2}}\delta(\omega-3\Omega) + e^{-3i(\tau_e-\gamma)-i\frac{\pi}{2}}\delta(\omega+3\Omega)\} \end{aligned} \tag{11}$$

Examining the expression for $L(\omega)$, it is noted that the solution contains components with frequencies at Ω and 3Ω. The amplitudes and phases of these components are given by

$$L(\Omega) = \frac{1}{2}ae^{i(\tau_e-\gamma)} \tag{12}$$

and

$$L(3\Omega) = \frac{a^3\alpha_v}{64\omega_s}e^{3i(\tau_e-\gamma)+i\frac{\pi}{2}} \tag{13}$$

The auto-trispectrum is then used to relate the two components, Ω and 3Ω. Using the definition of the trispectrum, we obtain

$$S_{lll}(\Omega,\Omega,\Omega) \approx \frac{a^6\alpha_v}{512\omega_s}e^{i\frac{\pi}{2}} \tag{14}$$

Equation 14 shows that the magnitude of the auto-trispectrum can be used to determine the coefficient of the cubic nonlinearity α_v. The phase of the auto-trispectrum $S_{lll}(\Omega,\Omega,\Omega)$, given by $\phi(3\Omega) - 3\phi(\Omega)$, and equal to $\frac{\pi}{2}$, should be used to establish the validity of the reduced-order model. The normalized auto-trispectrum, namely, the auto-tricoherence[6], should be used to determine the extent of cubic coupling between the two frequency components Ω and 3Ω and its level should be used to establish a level of confidence in the estimated values of the magnitude and phase of the auto-trispectrum and any derived parameters.

For the forced van der Pol equation with primary resonance, the steady state value of amplitude a and phase γ can be obtained by setting $\dot{a} = 0$ and $\dot{\gamma} = 0$ in Eq. 9, i.e.

$$\begin{aligned} 0 &= \tfrac{\mu_v}{2}a - \tfrac{\alpha_v}{8}a^3 + \tfrac{F}{2\omega_s}sin\gamma \\ 0 &= a\sigma - \tfrac{F}{2\omega_s}cos\gamma \end{aligned} \tag{15}$$

In order to determine the damping and nonlinear coefficients, and the external force parameters in the forced van der Pol equation from the amplitudes and phases of the Fourier components in the time series, the lift coefficient is written as

$$l(t) \approx acos(\Omega t + \tau_e - \gamma) + a_3cos(3(\Omega t + \tau_e - \gamma) + \tfrac{\pi}{2}) \tag{16}$$

By comparing Eq. 16 with Eq. 7, one obtains

$$\alpha_v = \frac{32\omega_s a_3}{a^3} \tag{17}$$

Alternatively and as explained above, α_v can be obtained from the magnitude of the auto-trispectrum. Rearranging Eq. 14, one obtains

$$\alpha_v = \frac{512\omega_s \left|S_{lll}(\omega_s, \omega_s, \omega_s)\right|}{a^6} \tag{18}$$

From the Fourier transform of $l(t)$ at frequency Ω, i.e. Eq. 12, one obtains

$$\tau_e - \gamma = \Phi(L(\Omega)) \tag{19}$$

where $\Phi(L(\Omega))$ is the phase angle of $L(\Omega)$. Therefore,

$$\gamma = \tau_e - \Phi(L(\Omega)) \tag{20}$$

Substituting Eq. 20 in Eq. 15 yields

$$F = \frac{(\Omega - \omega_s)2\omega_s a}{cos(\tau_e - \Phi(L(\Omega)))} \tag{21}$$

and

$$\mu_v = \frac{1}{4}\alpha_v a^2 + \frac{F}{a\omega_s} sin(\tau_e - \Phi(L(\Omega))) \tag{22}$$

Thus, given τ_e, one can identify F, and μ_v.

5 Results and Discussion

Vorticity contours in the wake of the cylinder subjected to rotational oscillations under lock-on conditions are presented in Fig.1. The figure clearly shows a vortex shedding pattern that is similar to the one observed when the cylinder is held stationary as presented in Fig. 2.

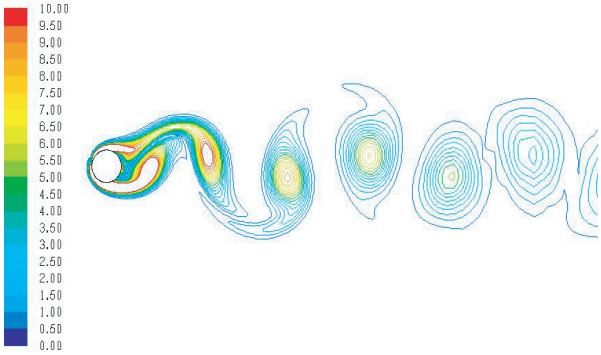

Figure 1: Vorticity contours in the wake of the rotationally oscillating cylinder. Forcing condition: $\dot{\theta}_{max}D/2U_\infty = 0.5., f_f U_\infty/D = 0.1643.$

The above notion is further strengthened by the lift and drag time series in the lock-on case, presented in Fig. 3. Both coefficients are characterized by perfect sinusoidal variations. The lift has a major frequency that corresponds to the vortex shedding frequency. The major frequency component in the drag is twice that of the lift. This sinusoidal behavior indicates a perfect vortex shedding as would be observed in the stationary case.

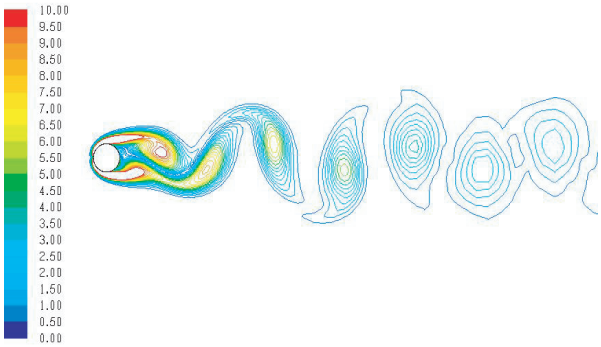

Figure 2: Vorticity contours in the wake of the stationary cylinder. $St = f_s U_\infty / D = 0.1747$.

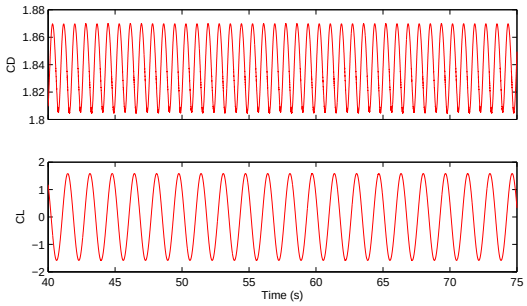

Figure 3: Time histories of the drag and lift coefficients on the rotationally oscillating cylinder. Forcing condition: $\dot{\theta}_{max} D/2U_\infty = 0.5., f_f U_\infty / D = 0.1643$.

Spectral analysis was performed on the lift time series that is plotted in Fig. 3. The power spectrum showed that the major frequency component is at that of the forcing frequency. Values of the spectral amplitudes at the vortex shedding frequency and its third harmonic were also determined from the power spectrum. These values were then used to determine α_v. The amplitude and phase of the auto-trispectrum were used to verify this value and to determine the phase relation between the vortex shedding component and its third harmonic. The phase γ was then determined. This value was used to determine F, and μ_v as explained above. The results are presented in Table 1.

van der Pol Parameter	Estimated Value
$\omega_s/2\ \pi$	0.1747
$\Omega/2\ \pi$	0.1643
μ_v	0.08408
α_v	0.1356
F	0.212
γ	0.0047 rad

Table 1: Estimated model parameters

Validation of the representative model and its parameters is demonstrated by comparing its integrated time series with the one obtained from the original numerical simulation. This com-

parison is presented in Fig. 4. Obviously, the derived model predicts the sinusoidal characteristic of the vortex shedding. This is further confirmed by the perfect matching of the amplitudes of the vortex shedding frequency and its third harmonic as obtained from the model and the numerical simulation as presented in Fig. 5. The observed difference at the high frequencies is relatively insignificant when comparing it with the spectral amplitudes of the vortex shedding frequency. This difference may be related to the level of accuracy in the integration of the analytical model.

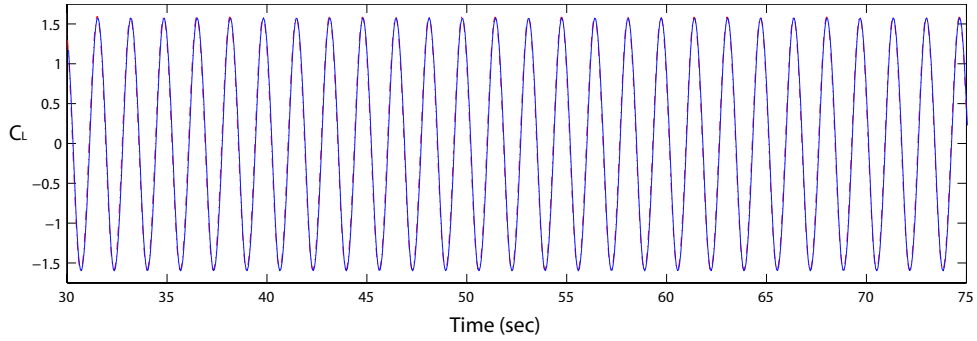

Figure 4: Comparison of the analytically modeled (blue line) and numerically simulated (red dashed line) lift time series.

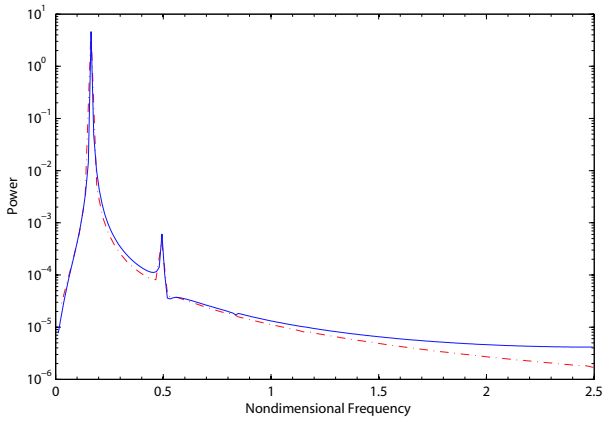

Figure 5: Comparison of the spectra of the analytically modeled (blue line) and numerically simulated (red dashed line) lift coefficients.

6 Conclusions

In this work, an analytical model for the prediction of the lift on a rotationally oscillating cylinder in the lock-on regime has been developed. The parameters of the developed model were determined from a numerical simulation of the flow field. Higher-order spectral analysis of the lift data yielded relevant quantities that were matched with approximate solutions of the assumed model. Based on this analysis, it is determined that the forced van der Pol equation could be used to model the lift coefficient on the rotationally oscillating cylinder in the lock-on regime. The validity of the model has been demonstrated by comparing time and frequency do-

main characteristics of the analytically modeled lift coefficient with the numerically simulated data.

REFERENCES

[1] P. T. Tokumaru and P. E. Dimotakis. Rotary oscillation control of a cylinder wake. *J. Fluid Mech.*, **224**, 77, 1991.

[2] X.-Y. Lu and J. Sato. A numerical study of flow past a rotationally oscillating circular cylinder. *J. Fluids Struct*, **10**, 829, 1996.

[3] M.-H. Chou. Synchronization of vortex shedding from a cylinder under rotary oscillation. *Comput. Fluids*, **26**, 755, 1997.

[4] S. Choi, K. Choi and S. Kang. Characteristics of flow over a rotationally oscillating cylinder at low Reynolds number. *Phys. of Fluids*, **14**(8), 2767, 2002.

[5] Hartlen, R. T. and Currie, I. G. Lift-Oscillator Model of Vortex-Induced Vibrations. *Journal of Engineering Mechanics*, **96**(5), 577, 1970.

[6] A. H. Nayfeh, F. Owis and M.R. Hajj. A model for the coupled lift and drag on a circular cylinder. *Proc. of DETC 2003, ASME* 19^{th} *Biennial Conference on Mechanical Vibrations and Noise*, Chicago, IL, USA, DETC2003/VIB-48455. 2003.

[7] Y.C. Kim and E. J. Powers. Digital bispectral analysis and its applications to nonlinear wave interactions. *IEEE Trans. Plasma Sci.*, **PS-7** 120-131, 1979.

[8] M. R. Hajj, R. W. Miksad and E. J. Powers. Fundamental-subharmonic interaction: effect of the phase relation. *Journal of Fluid Mechanics*, **256**, 403, 1993.

[9] M. R. Hajj, R. W. Miksad and E. J. Powers. Perspective: measurements and analysis of nonlinear wave interactions with higher-order spectral moments. *Journal of Fluids Engineering*, **119** 3, 1997.

[10] E. J. Powers and S. Im. Introduction to higher-order statistical signal processing and its applications. in: *Higher-Order Statistical Signal Processing* (Boashash, Powers & Zoubir eds.) Longman, Australia. 1995.

[11] A. H. Nayfeh *Perturbation Methods*, Wiley, New York. 1973.

[12] A. H. Nayfeh *Introduction to Perturbation Techniques*, Wiley, New York. 1981.